

Seismo Radial Grain Velocity Fractal Dimension for Characterizing Shajara Reservoirs of the Permo-Carboniferous Shajara Formation, Saudi Arabia

Khalid Elyas Mohamed Elameen Alkhidir

Department of Petroleum and Natural Gas Engineering, College of Engineering, King Saud University, Saudi Arabia

*Corresponding author

Prof. Khalid Elyas Mohamed Elameen Alkhidir, Ph.D. Department of Petroleum and Natural Gas Engineering, College of Engineering, King Saud University, Saudi Arabia

Submitted: 22 Dec 2019; Accepted: 02 Jan 2020; Published: 06 Feb 2020

Abstract

The quality and assessment of a reservoir can be documented in details by the application of seismo radial grain velocity. This research aims to calculate fractal dimension from the relationship among seismo radial grain velocity, maximum seismo radial grain velocity and wetting phase saturation and to approve it by the fractal dimension derived from the relationship among capillary pressure and wetting phase saturation. Two equations for calculating the fractal dimensions have been employed. The first one describes the functional relationship between wetting phase saturation, seismo radial grain velocity, maximum seismo radial grain velocity and fractal dimension. The second equation implies to the wetting phase saturation as a function of capillary pressure and the fractal dimension. Two procedures for obtaining the fractal dimension have been utilized. The first procedure was done by plotting the logarithm of the ratio between seismo radial grain velocity and maximum seismo radial grain velocity versus logarithm wetting phase saturation. The slope of the first procedure = $3 - D_f$ (fractal dimension). The second procedure for obtaining the fractal dimension was determined by plotting the logarithm of capillary pressure versus the logarithm of wetting phase saturation. The slope of the second procedure = $D_f - 3$. On the basis of the obtained results of the fabricated stratigraphic column and the attained values of the fractal dimension, the sandstones of the Shajara reservoirs of the Shajara Formation were divided here into three units.

Keywords: Shajara Reservoirs, Shajara Formation, Seismo radial grain velocity fractal dimension, Capillary pressure fractal dimension

Introduction

Seismo electric effects related to electro kinetic potential, dielectric permittivity, pressure gradient, fluid viscosity, and electric conductivity was first reported [1]. Capillary pressure follows the scaling law at low wetting phase saturation was reported [2]. Seismo electric phenomenon by considering electro kinetic coupling coefficient as a function of effective charge density, permeability, fluid viscosity and electric conductivity was reported [3]. The magnitude of seismo electric current depends on porosity, pore size, zeta potential of the pore surfaces, and elastic properties of the matrix was investigated [4]. The tangent of the ratio of converted electric field to pressure is approximately in inverse proportion to permeability was studied [5]. Permeability inversion from seismoelectric log at low frequency was studied [6]. They reported that, the tangent of the ratio among electric excitation intensity and pressure field is a function of porosity, fluid viscosity, frequency, tortuosity and fluid density and Dracy permeability. A decrease of seismo electric frequencies with increasing water content was reported by [7]. An increase of seismo electric transfer function with increasing water saturation was studied by [8]. An increase of dynamic seismo electric transfer

function with decreasing fluid conductivity was described by [9]. The amplitude of seismo electric signal increases with increasing permeability which means that the seismo electric effects are directly related to the permeability and can be used to study the permeability of the reservoir was illustrated by [10]. Seismo electric coupling is frequency dependent and decreases exponentially when frequency increases was demonstrated by [11]. An increase of permeability with increasing pressure head and bubble pressure fractal dimension was reported by [12,13]. An increase of geometric relaxation time of induced polarization fractal dimension with permeability increasing and grain size was described by [14,15].

Material and Method

Sandstone samples were collected from the surface type section of the Permo-Carboniferous Shajara Formation, latitude $26^{\circ} 52' 17.4''$, longitude $43^{\circ} 36' 18''$. (Figure1). Porosity was measured on collected samples using mercury intrusion Porosimetry and permeability was derived from capillary pressure data. The purpose of this paper is to obtain seismo radial grain velocity fractal dimension and to confirm it by capillary pressure fractal dimension. The fractal dimension of the first procedure is determined from the positive slope of the plot of logarithm of the ratio of seismo radial grain velocity to maximum seismo radial grain velocity log ($SRGV^{1/4}/SRGV_{max}^{1/4}$) versus log

wetting phase saturation (logSw). Whereas the fractal dimension of the second procedure is determined from the negative slope of the plot of logarithm of log capillary pressure (log Pc) versus logarithm of wetting phase saturation (log Sw).

AGE	Fm.	Mbr.	unit	LITHO-LOGY	DESCRIPTION
Late Permian	Khuff Formation	Huqf1 Member			Limestone : Cream, dense, burrowed, thickness 6.5'
					Sub-Khuff unconformity.
		Upper Shajara Member	Upper Shajara Reservoir		Mudstone : Yellow, thickness 17.7'
				SJ13▲	Sandstone : Light brown, cross-bedded, coarse-grained, poorly sorted, porous, friable, thickness 6.5'
				SJ12▲	
				SJ11▲	Sandstone : Yellow, medium-grained, very coarse-grained, poorly, moderately sorted, porous, friable, thickness 13.1'
		Middle Shajara Member	Middle Shajara Reservoir		Mudstone : Yellow-green, thickness 11.8'
					Mudstone : Yellow, thickness 1.3'
					Mudstone : Brown, thickness 4.5'
				SJ10▲	Sandstone : Light brown, medium-grained, moderately sorted, porous, friable, thickness 3.0'
				SJ9▲	Sandstone : Yellow, medium-grained, moderately well sorted, porous, friable, thickness 0.9'
				SJ8▲	
				SJ7▲	Sandstone : Red, coarse-grained, medium-grained, moderately well sorted, porous, friable, thickness 13.4'
		Lower Shajara Member	Lower Shajara Reservoir		
				SJ6▲	Sandstone : White with yellow spots, fine-grained, hard, thickness 2.6'
				SJ5▲	Sandstone : Limonite, thickness 1.3'
				SJ4▲	Sandstone : White, coarse-grained, very poorly sorted, thickness 4.5'
				SJ3▲	Sandstone : White-pink, poorly sorted, thickness 1.0'
				SJ2▲	Sandstone : Yellow, medium-grained, well sorted, porous, friable, thickness 3.9'
				SJ1▲	
					Sandstone : Red, medium-grained, moderately well sorted, porous, friable, thickness 11.8'
Early Devonian	Ta'if Formation				Sub-Ulayzah unconformity. Sandstone : White, fine-grained.

Figure 1: Surface type section of the Shajara Reservoirs of the Permo-Carboniferous Shajara Formation at latitude 26° 52' 17.4" longitude 43° 36' 18"

The Seismo radial grain velocity can be scaled as

$$Sw = \left[\frac{SRGV^{\frac{1}{4}}}{SRGV_{max}^{\frac{1}{4}}} \right]^{[3-Df]} \quad (1)$$

Where Sw the water saturation, SRGV the seismo radial grain velocity in meter / second, SRGV_{max} the maximum seismo radial grain velocity in meter / second, and Df the fractal dimension.

Equation 1 can be proofed from

$$H = \left[\frac{\phi * \epsilon * kf * \zeta * \rho f * SSWV * SRGV}{\alpha_{\infty} * \eta} \right] \quad (2)$$

Where H the magnetic field in ampere / meter, ϕ the porosity, ϵ the fluid permittivity in Faraday / meter, kf the fluid dielectric constant, the fluid density Pf in kilogram / cubic meter, SSWV the seismic shear wave velocity in meter / second, SRGV the seismo radial grain velocity in meter / second, α the tortuosity, η the fluid viscosity in pascal * second

The fluid density Pf can be scaled as

$$Pf = \left[\frac{m}{V} \right] \quad (3)$$

Where Pf the fluid density Pf in kilogram / cubic meter, m the mass in kilogram, V the volume in cubic meter
Insert equation 3 into equation 2

$$H = \left[\frac{\phi * \epsilon * kf * \zeta * m * SSWV * SRGV}{\alpha_{\infty} * \eta * V} \right] \quad (4)$$

The volume can be scaled as

$$V = Q * t \quad (5)$$

Where V the volume in cubic meter, Q the flow rate in cubic meter/ second, t the time in second

Insert equation 5 into equation 4

$$H = \left[\frac{\phi * \epsilon * kf * \zeta * m * SSWV * SRGV}{\alpha_{\infty} * \eta * Q * t} \right] \quad (6)$$

The rate Q can be scaled as

$$Q = \left[\frac{3.14 * r^4 * \Delta p}{8 * \eta * L} \right] \quad (7)$$

Where Q the flow rate in cubic meter / second, r the pore radius in meter, Δp the differential pressure in pascal, η the fluid viscosity in pascal * second, L the capillary length in meter.

Insert equation 7 into equation 6

$$H = \left[\frac{\phi * \epsilon * kf * \zeta * m * 8 * \eta * L * SSWV * SRGV}{\alpha_{\infty} * \eta * 3.14 * r^4 * \Delta p * t} \right] \quad (8)$$

Equation 8 after rearrange will become

$$H * r^4 = \left[\frac{\phi * \epsilon * kf * \zeta * m * 8 * \eta * L * SSWV * SRGV}{\alpha_{\infty} * \eta * 3.14 * \Delta p * t} \right] \quad (9)$$

The maximum pore radius can be scaled as

$$H * r_{max}^4 = \left[\frac{\phi * \epsilon * kf * \zeta * m * 8 * \eta * L * SSWV * SRGV_{max}}{\alpha_{\infty} * \eta * 3.14 * \Delta p * t} \right] \quad (10)$$

Divide equation 9 by equation 10

$$\frac{H * r^4}{H * r_{max}^4} = \left[\frac{\left[\frac{\phi * \epsilon * kf * \zeta * m * 8 * \eta * L * SSWV * SRGV}{\alpha_{\infty} * \eta * 3.14 * \Delta p * t} \right]}{\left[\frac{\phi * \epsilon * kf * \zeta * m * 8 * \eta * L * SSWV * SRGV_{max}}{\alpha_{\infty} * \eta * 3.14 * \Delta p * t} \right]} \right] \quad (11)$$

Equation 11 after simplification will become

$$\left[\frac{r^4}{r_{max}^4} \right] = \left[\frac{SRGV}{SRGV_{max}} \right] \quad (12)$$

Take the fourth root of equation 12

$$\sqrt[4]{\left[\frac{r^4}{r_{max}^4} \right]} = \sqrt[4]{\left[\frac{SRGV}{SRGV_{max}} \right]} \quad (13)$$

Equation 13 after simplification will become

$$\left[\frac{r}{r_{\max}} \right] = \left[\frac{SRGV^{\frac{1}{4}}}{SRGV_{\max}^{\frac{1}{4}}} \right] \quad (14)$$

Take the logarithm of equation 14

$$\log \left[\frac{r}{r_{\max}} \right] = \log \left[\frac{SRGV^{\frac{1}{4}}}{SRGV_{\max}^{\frac{1}{4}}} \right] \quad (15)$$

$$\text{But; } \log \left[\frac{r}{r_{\max}} \right] = \left[\frac{\log Sw}{3 - Df} \right] \quad (16)$$

Insert equation 16 into equation 15

$$\left[\frac{\log Sw}{3 - Df} \right] = \log \left[\frac{SRGV^{\frac{1}{4}}}{SRGV_{\max}^{\frac{1}{4}}} \right] \quad (17)$$

Equation 17 after log removal will become

$$Sw = \left[\frac{SRGV^{\frac{1}{4}}}{SRGV_{\max}^{\frac{1}{4}}} \right]^{[3 - Df]} \quad (18)$$

Equation 18 the proof of equation 1 which relates the water saturation, seismo radial grain velocity, maximum seismo radial grain velocity, and the fractal dimension. The capillary pressure can be scaled as

$$\text{LogSw} = [Df - 3] * \log pc + \text{constant} \quad (19)$$

Where Sw the water saturation, Pc the capillary pressure and Df the fractal dimension.

Results and Discussion

Based on field observation the Shajara Reservoirs of the Permo-Carboniferous Shajara Formation were divided here into three units as described in (Figure1). These units from bottom to top are: Lower Shajara Reservoir, Middle Shajara reservoir, and Upper Shajara Reservoir. Their attained results of the seismo radial grain velocity fractal dimension and capillary pressure fractal dimension are shown in Table 1. Based on the achieved results it was found that the seismo radial grain velocity fractal dimension is equal to the capillary pressure fractal dimension. The maximum value of the fractal dimension was found to be 2.7872 allocated to sample SJ13 from the Upper Shajara Reservoir as verified in Table 1. Whereas the minimum value of the fractal dimension 2.4379 was reported from sample SJ3 from the Lower Shajara reservoir as shown in Table1. The Seismo radial grain velocity fractal dimension and capillary pressure fractal dimension were detected to increase with increasing permeability as proofed in Table1 owing to the possibility of having interconnected channels.

Table 1: Petrophysical model showing the three Shajara Reservoir Units with their corresponding values of seismo radial grain velocity fractal dimension and capillary pressure fractal dimension

Formation	Reservoir	Sample	Porosity %	k (md)	Positive slope of the first procedure Slope=3-Df	Negative slope of the second procedure Slope=Df-3	Seismo radial grain velocity fractal dimension	Capillary pressure fractal dimension
Permo-Carboniferous Shajara Formation	Upper	SJ13	25	973	0.2128	-0.2128	2.7872	2.7872
	Shajara	SJ12	28	1440	0.2141	-0.2141	2.7859	2.7859
	Reservoir	SJ11	36	1197	0.2414	-0.2414	2.7586	2.7586
	Middle	SJ9	31	1394	0.2214	-0.2214	2.7786	2.7786
	Shajara	SJ8	32	1344	0.2248	-0.2248	2.7752	2.7752
	Reservoir	SJ7	35	1472	0.2317	-0.2317	2.7683	2.7683
	Lower	SJ4	30	176	0.3157	-0.3157	2.6843	2.6843
	Shajara	SJ3	34	56	0.5621	-0.5621	2.4379	2.4379
	Reservoir	SJ2	35	1955	0.2252	-0.2252	2.7748	2.7748
		SJ1	29	1680	0.2141	-0.2141	2.7859	2.7859

The Lower Shajara reservoir was symbolized by six sandstone samples (Figure 1), four of which label as SJ1, SJ2, SJ3 and SJ4 were carefully chosen for capillary pressure measurement as proven in Table1. Their positive slopes of the first procedure log of the Seismo radial grain velocity to maximum Seismo radial grain velocity versus log wetting phase saturation (Sw) and negative slopes of the second procedure log capillary pressure (Pc) versus log wetting phase saturation (Sw) are clarified in (Figure 2,3,4,5 & Table 1). Their Seismo radial grain velocity fractal dimension and capillary pressure fractal dimension values are revealed in Table 1. As we proceed from sample SJ2 to SJ3 a pronounced reduction in permeability due to compaction was described from 1955 md to 56 md which reflects decrease in Seismo radial grain velocity fractal dimension from 2.7748 to 2.4379 as quantified in table 1. Again, an increase in grain size and permeability was proved from sample SJ4 whose seismo radial grain velocity fractal dimension and capillary pressure fractal dimension was found to be 2.6843 as described in Table 1.

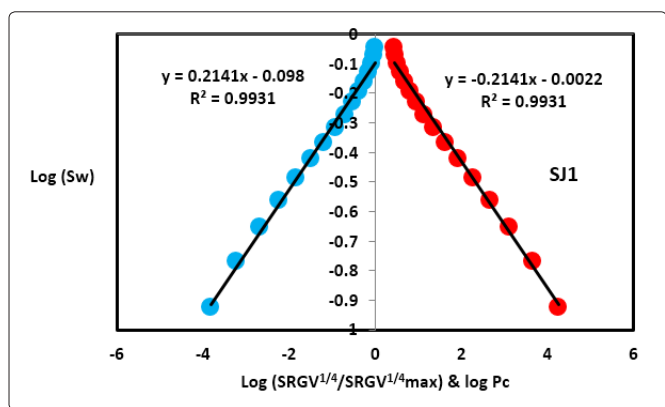


Figure 2: Log (SRGV1/4/SRGV1/4max) & log pc versus log Sw for sample SJ1

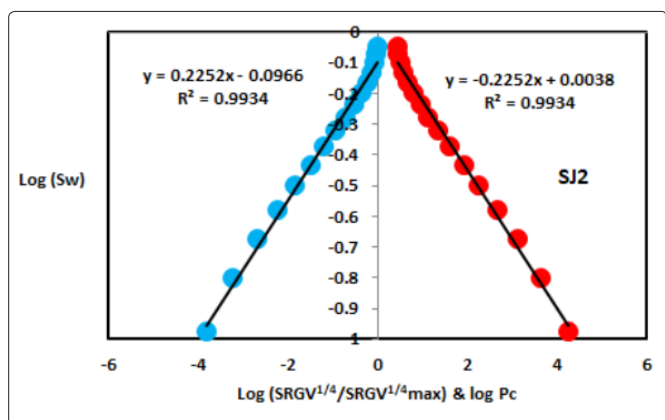


Figure 3: Log (SRGV1/4/SRGV1/4max) & log pc versus log Sw for sample SJ2

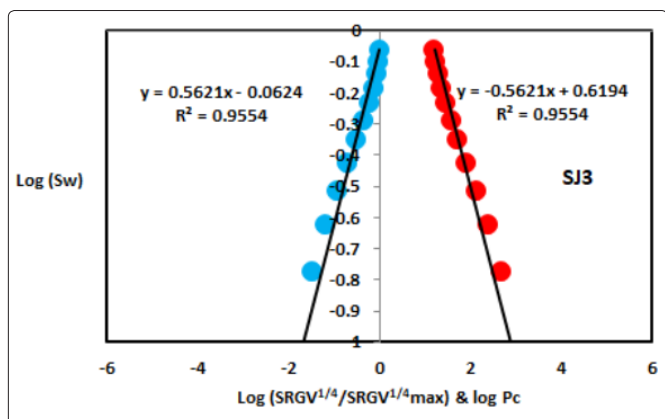


Figure 4: Log (SRGV1/4/SRGV1/4max) & log pc versus log Sw for sample SJ3

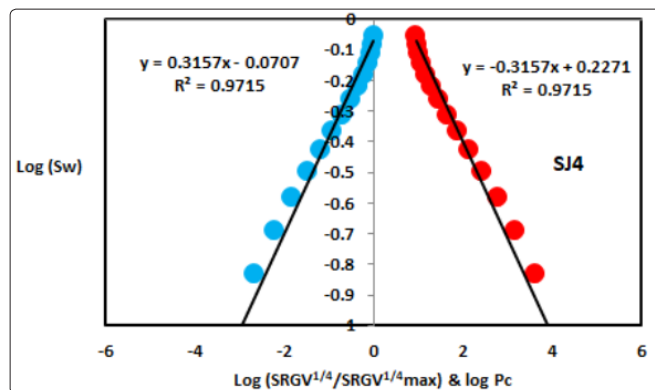


Figure 5: Log (SRGV1/4/SRGV1/4max) & log pc versus log Sw for sample SJ4

In contrast, the Middle Shajara reservoir which is separated from the Lower Shajara reservoir by an unconformity surface as revealed in (Figure 1). It was nominated by four samples (Figure 1), three of which named as SJ7, SJ8, and SJ9 as illuminated in Table 1 were chosen for capillary measurements as described in Table 1. Their positive slopes of the first procedure and negative slopes of the second procedure are shown in (Figure 6, 7 & 8 and Table 1). Furthermore, their Seismo radial grain velocity fractal dimensions and capillary pressure fractal dimensions show similarities as defined in Table 1. Their fractal dimensions are higher than those of samples SJ3 and SJ4 from the Lower Shajara Reservoir due to an increase in their permeability as explained in table 1.

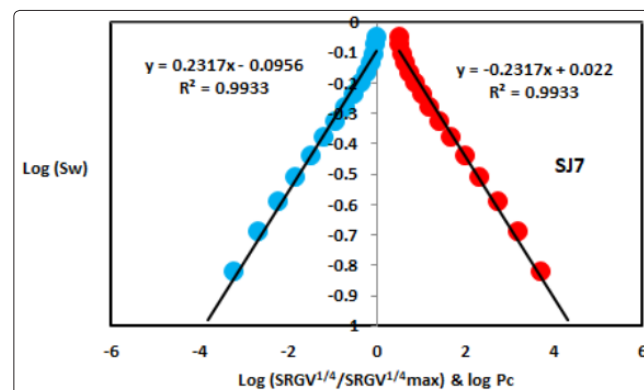


Figure 6: Log (SRGV1/4/SRGV1/4max) & log pc versus log Sw for sample SJ7

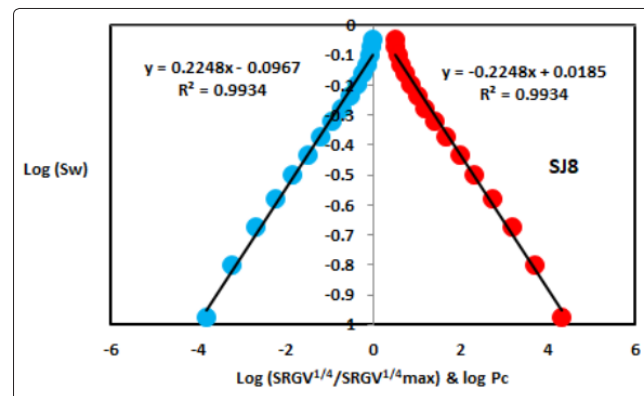


Figure 7: Log (SRGV1/4/SRGV1/4max) & log pc versus log Sw for sample SJ8

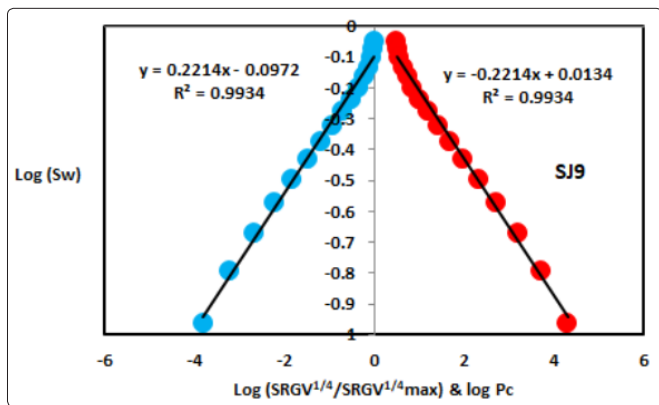


Figure 8: Log (SRGV^{1/4}/SRGV^{1/4max}) & log pc versus log Sw for sample SJ9

On the other hand, the Upper Shajara reservoir was separated from the Middle Shajara reservoir by yellow green mudstone as shown in (Figure 1). It is defined by three samples so called SJ11, SJ12, SJ13 as explained in Table 1. Their positive slopes of the first procedure and negative slopes of the second procedure are displayed in (Figure 9, 10 & 11 and Table 1). Moreover, their seismo radial grain velocity fractal dimension and capillary pressure fractal dimension are also higher than those of sample SJ3 and SJ4 from the Lower Shajara Reservoir due to an increase in their permeability as simplified in table 1.

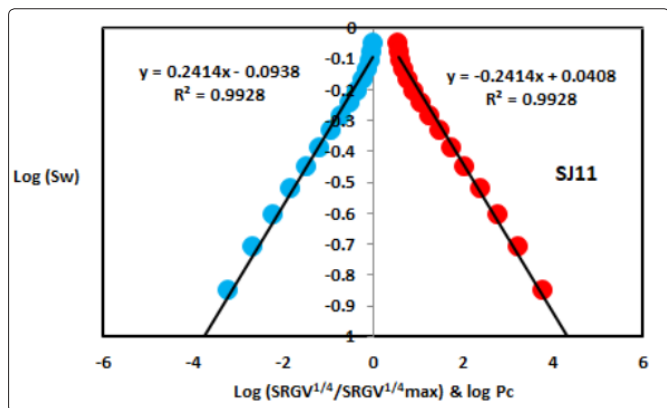


Figure 9: Log (SRGV^{1/4}/SRGV^{1/4max}) & log pc versus log Sw for sample SJ11

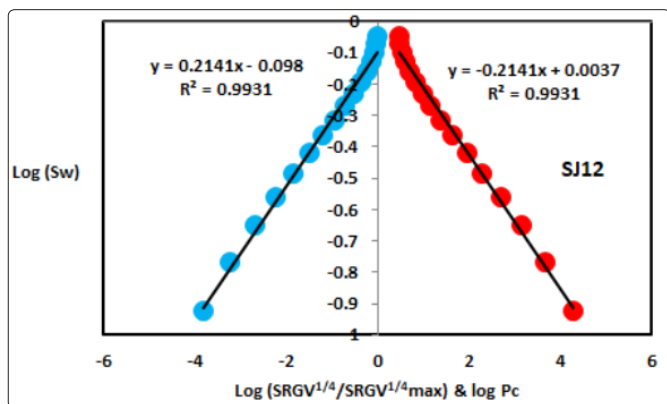


Figure 10: Log (SRGV^{1/4}/SRGV^{1/4max}) & log pc versus log Sw for sample SJ12

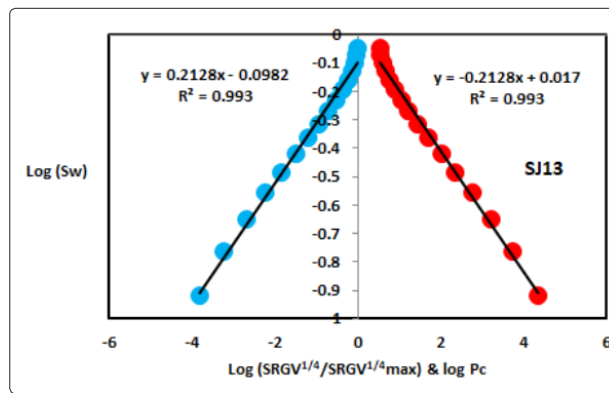


Figure 11: Log (SRGV^{1/4}/SRGV^{1/4max}) & log pc versus log Sw for sample SJ13

Overall a plot of positive slope of the first procedure versus negative slope of the second procedure as described in (Figure 12) reveals three permeable zones of varying Petrophysical properties. These reservoir zones were also confirmed by plotting seismo radial grain velocity fractal dimension versus capillary pressure fractal dimension as described in (Figure 13). Such variation in fractal dimension can account for heterogeneity which is a key parameter in reservoir quality assessment.

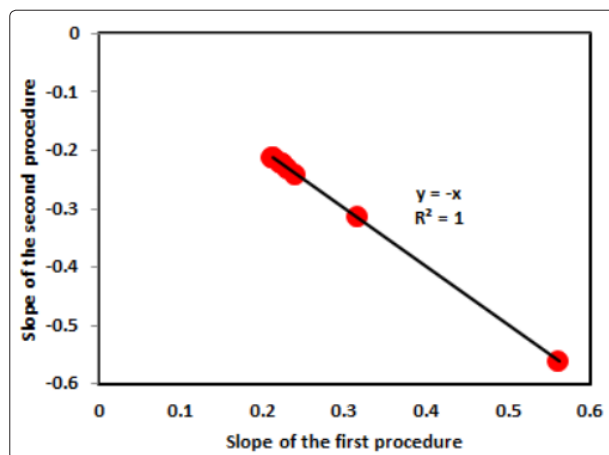


Figure 12: Slope of the first procedure versus slope of the second procedure

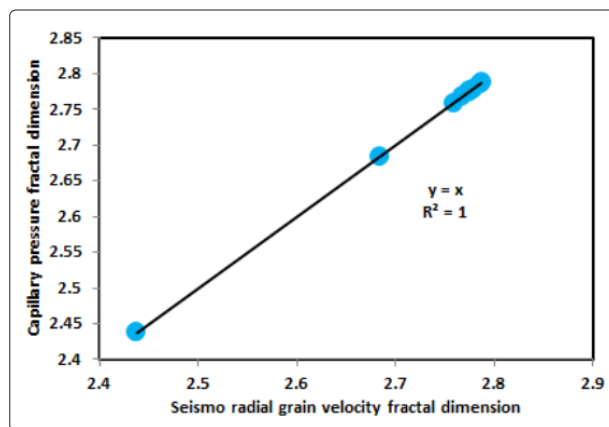


Figure 13: Seismo radial grain velocity fractal dimension versus capillary pressure fractal dimension

Conclusion

The sandstones of the Shajara Reservoirs of the permo-Carboniferous Shajara Formation were divided here into three units based on seismo radial grain velocity fractal dimension. The Units from base to top are: Lower Shajara Seismo Radial Grain Velocity Fractal Dimension Unit, Middle Shajara Seismo Radial Grain Velocity Fractal Dimension Unit, and Upper Shajara Seismo Radial Grain Velocity Fractal Dimension Unit. These units were also proved by capillary pressure fractal dimension. The fractal dimension was found to increase with increasing grain size and permeability owing to possibility of having interconnected channels.

Acknowledgement

The author would to thank King Saud University, college of Engineering, Department of Petroleum and Natural Gas Engineering, Department of Chemical Engineering, Research Centre at College of Engineering, College of science, Department of Geology, and King Abdullah Institute for research and Consulting Studies for their supports.

References

1. Frenkel J (1944) On the theory of seismic and seismoelectric phenomena in a moist soil. *Journal of physics* 3: 230-241.
2. Li Kewen, Williams Wade (2007) Determination of capillary pressure function from resistivity data. *Transport in Porous Media* 67: 1-15.
3. Revil A, Jardani A (2010) Seismo electric response of heavy oil reservoirs: theory and numerical modelling. *Geophysical J International* 180: 781-797.
4. Dukhin A, Goetz P, Thommes M (2010) Seismoelectric effect: a non-isochoric streaming current.1 Experiment. *J Colloid Interface Sci* 345: 547-553.
5. Guan W, Hu H, Wang Z (2013) Permeability inversion from low-frequency seismoelectric logs in fluid-saturated porous formations. *Geophys Prospect* 61: 120-133.
6. Hu H, Guan W, Zhao W (2012) Theoretical studies of permeability inversion from seismoelectric logs. *Geophysical Research Abstracts* 14: EGU General Assembly, p 6725.
7. Borde C, Senechal P, Barriere J, Brito D, Normandin E, et al. (2015) Impact of water saturation on seismoelectric transfer functions: a laboratory study of co-seismic phenomenon. *Geophysical J International* 200: 1317-1335.
8. Jardani A, Revil A (2015) Seismoelectric couplings in a poroelastic material containing two immiscible fluid phases. *Geophysical Journal International* 202: 850-870.
9. Holzhauser J, Brito D, Bordes C, Brun Y, Guatarbes B (2016) Experimental quantification of the seismoelectric transfer function and its dependence on conductivity and saturation in loose sand. *Geophys Prospect* 65: 1097-1120
10. Rong Peng, Jian-Xing Wei, Bang-Rang Di, Pin-Bo Ding, Zi Chun Liu (2016) Experimental research on seismoelectric effects in sandstone. *Applied Geophysics* 13: 425-436.
11. Djuraev U, Jufar S R, Vasant P (2017) Numerical Study of frequency-dependent seismo electric coupling in partially saturated porous media. *MATEC Web of Conferences* 87, 02001.
12. Alkhidir KEME (2017) Pressure head fractal dimension for characterizing Shajara Reservoirs of the Shajara Formation of the Permo-Carboniferous Unayzah Group, Saudi Arabia. *Arch Pet Environ Bio techno* 12: 1-7.
13. Al-Khidir KE (2018) On Similarity of Pressure Head and Bubble Pressure Fractal Dimensions for Characterizing Permo Carboniferous Shajara Formation, Saudi Arabia. *J Indust Pollut Toxic* 1: 1-10.
14. Alkhidir KEME (2018) Geometric relaxation time of induced polarization fractal dimension for characterizing Shajara Reservoirs of the Shajara Formation of the Permo-Carboniferous Unayzah Group, Saudi Arabia, *Scifed J Petroleum* 2: 1-6.
15. Alkhidir KEME (2018) Geometric relaxation time of induced polarization fractal dimension for characterizing Shajara Reservoirs of the Shajara formation of the Permo-Carboniferous Unayzah Group-Permo. *Int J Pet and Res* 2: 105-108.

Copyright: ©2020 Khalid Elyas Mohamed Elameen Alkhidir. This is an open-access article distributed under the terms of the Creative Commons Attribution License, which permits unrestricted use, distribution, and reproduction in any medium, provided the original author and source are credited.